Received: 28 February 2020 | Revised: 5 May 2020 | Accepted: 30 May 2020

DOI: 10.1002/ptr.6780

RESEARCH ARTICLE

WILEY

Curcumin downregulates the PI3K–AKT–mTOR pathway and inhibits growth and progression in head and neck cancer cells

Gabriel Alvares Borges[1,2] | Silvia Taveira Elias[2] | Bruna Amorim[2] | Caroline Lourenço de Lima[2] | Ricardo Della Coletta[3] | Rogerio Moraes Castilho[1] | Cristiane Helena Squarize[1] | Eliete Neves Silva Guerra[1,2]

[1]Epithelial Biology Laboratory, Department of Periodontics and Oral Medicine, Division of Oral Pathology Oral Radiology and Oral Medicine, University of Michigan School of Dentistry, Ann Arbor, Michigan

[2]Laboratory of Oral Histopathology, Health Sciences Faculty, University of Brasilia, Brazil

[3]Department of Oral Diagnosis, School of Dentistry, University of Campinas, Piracicaba, Brazil

Correspondence
Eliete Neves Silva Guerra, Laboratory of Oral Histopathology, Health Sciences Faculty, University of Brasilia, Brasília, DF, 70910-900, Brazil.
Email: elieteneves@unb.br

Funding information
CNPq - National Council for Scientific and Technological Development, Brazil, Grant/Award Number: 140507/2016-7; CAPES - Coordination for the Improvement of Higher Education Personnel, Brazil, Grant/Award Number: 88881.187926/2018-01; Foundation of the Federal District-FAPDF, Grant/Award Number: 00193.00002099/2018-65; DPI-UnB N04/2019: 33902001.

Abstract

Curcumin, a polyphenol isolated from the rhizome of *Curcuma longa*, has been studied because of its antioxidant, antimicrobial, and antiinflammatory properties. This study aimed to evaluate the effects of curcumin on head and neck cancer (HNC) cell lines and how it modulates the PI3K–AKT–mTOR signaling pathway. Dose-response curves for curcumin were established for hypopharynx carcinoma (FaDu), tongue carcinoma (SCC-9), and keratinocytes (HaCaT) cell lines and IC_{50} values were calculated. Cell cycle and cell death were investigated through flow cytometry. Cytoskeleton organization was assessed through phalloidin+FITC staining. qPCR array and western blot were performed to analyze gene and protein expression. Curcumin reduced cell viability in a dose-dependent and selective manner, induced cell death on SCC-9 cells (necrosis/late apoptosis: 44% curcumin vs. 16.4% vehicle), and arrested cell cycle at phase G_2/M on SCC-9 and FaDu (G_2: SCC-9—19.1% curcumin vs. 13.4% vehicle; FaDu—37.8% curcumin vs. 12.9% vehicle). Disorganized cytoskeleton and altered cell morphology were observed. Furthermore, curcumin downregulated the PI3K–AKT–mTOR signaling pathway by modifying the expression of key genes and proteins. These findings highlight the promising therapeutic potential of curcumin to inhibit HNC growth and progression and to modulate the PI3K–AKT–mTOR pathway.

KEYWORDS
cell cycle, cell death, curcumin, cytoskeleton, head and neck cancer, PI3K–AKT–mTOR pathway

1 | INTRODUCTION

Curcumin is a natural polyphenol isolated from *Curcuma longa* that has been extensively studied in the past years, mostly because of its antioxidant, antimicrobial, and antiinflammatory properties (Edwards et al., 2017; Kahkhaie et al., 2019; Kotha & Luthria, 2019). Such effects might be explained by its ability to interact with different transcription factors, inflammatory mediators, and protein kinases, and therefore modulate signaling pathways that are linked to several disorders (Kahkhaie et al., 2019; Kunnumakkara et al., 2017; Normando et al., 2019). A recent overview identified 22 systematic reviews that reported the clinical efficacy of curcumin-containing nutraceuticals in metabolic and inflammatory-related diseases; however, due to the poor quality of the primary trials and the low-to-moderate level of reviews, there is still some uncertainty (Izzo, 2020; Pagano, Romano, Izzo, & Borrelli, 2018). Curcumin has also been reported as a potential antitumor agent, being active against different types of cancer (Lin et al., 2020; Saadipoor et al., 2019; Willenbacher et al., 2019).

As reported by the GLOBOCAN 2018, the global incidence for oral cavity, oropharynx, and hypopharynx cancers combined was

estimated at 528,359 in 2018 (Bray et al., 2018). The head and neck squamous cell carcinoma (HNSCC) is the most frequent head and neck cancer (HNC), and it is associated with the use of tobacco and alcohol, as well as the infection with oncogenic subtypes of human papillomavirus (HPV) (Cramer, Burtness, Le, & Ferris, 2019). Treatment depends on the stage of the disease, and surgery is frequently employed, followed by radiotherapy, chemotherapy, or a combination of those approaches (Cramer et al., 2019). The mortality and the morbidity associated with the treatment of HNC are still a concern, despite remarkable advances in the field, such as targeted therapy,

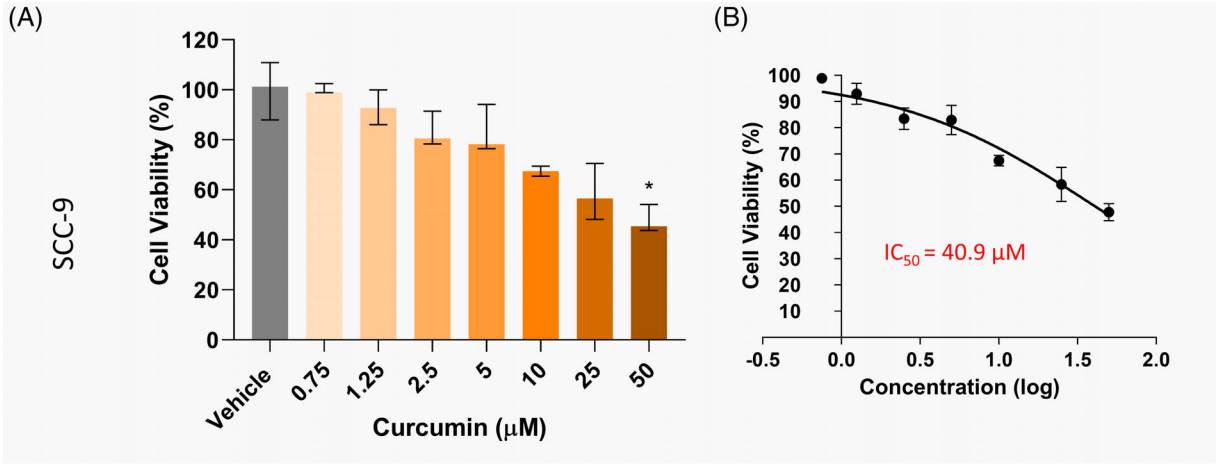

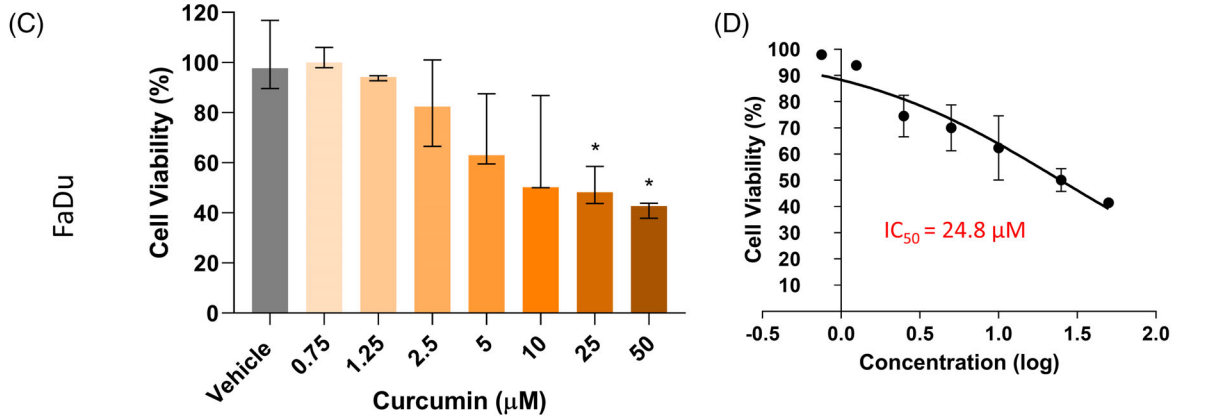

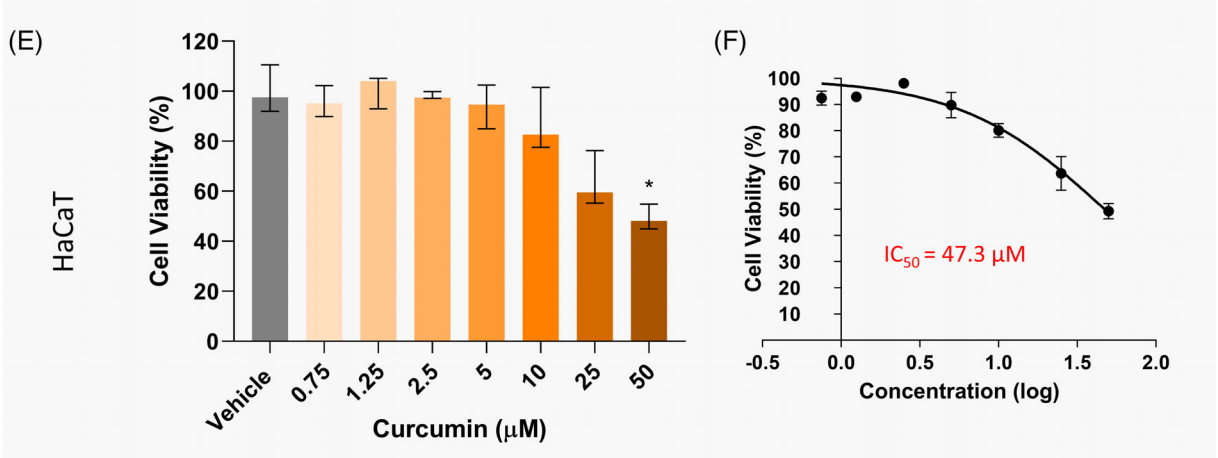

(G)

$$\text{Tumor Selectivity Index (TSI)} = \frac{IC_{50}\ HaCaT}{IC_{50}\ Tumor\ cell\ line}$$

Cell Line	TSI
SCC-9	1.15
FaDu	1.91

FIGURE 1 Legend on next page.

immunotherapy, and technological developments in surgery and radiotherapy (Cramer et al., 2019).

The phosphoinositide-3-kinase (PI3K)–protein kinase B (AKT)–mechanistic target of rapamycin (mTOR) signaling pathway regulates many cellular processes that ultimately relate to cell growth and proliferation (Murugan, 2019). This signaling pathway is found deregulated in cancer, which is characterized by an overexpression/hyperactivation of its effector proteins and alterations (amplification and mutation) on genes that encode those proteins (Murugan, 2019). This deregulation results in cell survival, cytoskeleton rearrangement, invasion, metastasis, and evasion of apoptosis (Murugan, 2019).

In a systematic review regarding the effects of curcumin on in vitro and in vivo HNC models, curcumin was reported to significantly reduce cell viability and tumor growth, inhibit cell proliferation, and induce cell cycle arrest and apoptosis (Borges et al., 2017). Recent studies showed that curcumin inhibited the activity of the mTOR complex 1 (mTORC1) on erythroleukemia cell lines (Petiti et al., 2019) and significantly decreased the expression and phosphorylation of AKT and mTOR on lung cancer (Liu et al., 2018) and ovarian cancer cells (Liu et al., 2019). It also reduced the phosphorylated levels of the downstream effectors ribosomal protein S6 kinase (p70 S6K) and 4E-binding protein 1 (4E-BP1) on ovarian cancer cells (Liu et al., 2019).

Therefore, the objectives of this study were to provide new biological insights into the effects of curcumin on two different HNC cell lines (SCC-9 and FaDu) and to demonstrate how it modulates the PI3K–AKT–mTOR signaling pathway.

2 | MATERIALS AND METHODS

2.1 | Curcumin

Curcumin was purchased from Sigma-Aldrich (St. Louis, Missouri—Reference: #08511). Stock solution was prepared by diluting 10 mg in DMSO to the concentration of 25 mM, and stored, protected from light, at −80°C until it was used.

2.2 | Cell culture

Three human cell lines were used for the experiments: SCC-9 (tongue squamous cell carcinoma), FaDu (hypopharynx squamous cell carcinoma), and HaCaT (human keratinocytes). SCC-9 cells were cultured in 1:1 Dulbecco's modified Eagle medium (DMEM)/F12 with 10% fetal bovine serum (FBS), 1% antibiotics (penicillin–streptomycin), and 400 ng/ml hydrocortisone. FaDu and HaCaT wells were cultured in DMEM supplemented with 10% FBS and 1% antibiotics. Cells were incubated in 5% CO_2 at 37°C. Cell culture reagents were purchased from Sigma-Aldrich. The cell lines are described in the American Type Culture Collection (ATCC), and they were used for the experiments on the third–fifth passage after thawing.

2.3 | Cell viability assay—Dose-response curves

Cells were seeded into 96-well plates at a density of 5×10^3 cells/well, incubated overnight and treated with curcumin (50, 25, 10, 5, 2.5, 1.25, or 0.75 μM) for 24 and 48 hrs. After treatment, 10 μl of MTT solution (3-[4,5-dimethyl-2-thiazolyl]-2,5-diphenyl-2*H*-tetrazolium bromide) (Sigma-Aldrich) at 5 mg/ml was added to each well, followed by incubation for 4 hr at 37°C. Medium was aspirated, and 100 μl of acidified isopropanol was added to dissolve formazan crystals. Absorbance was measured at 570 nm in a DTX 800 reader (Beckman Coulter, California).

The half-maximal inhibitory concentrations (IC_{50}) were estimated based on the dose-response curves, and the Tumor Selectivity Index (TSI) was calculated according to the formula: $\text{TSI} = \frac{IC_{50}\ \text{Control cell(HaCaT)}}{IC_{50}\ \text{Tumor cell(SCC}-9\ \text{or FaDu)}}$. Further experiments were performed with curcumin at IC_{50} concentrations.

2.4 | Cell cytometry—Cell cycle and cell death

For the cell cycle assay, cells were seeded into six-well plates at a density of 2×10^5 cells/well and incubated overnight. SCC-9 and FaDu cells were incubated in medium without FBS for 24 and 48 hrs before treatment, respectively. Curcumin was diluted in medium with FBS and added to the wells. After 24 hrs of treatment, cells were collected, fixated on 70% ethanol and kept at −20°C until the assay. Cells were stained with propidium iodide (Sigma-Aldrich) at 50 μg/ml and assessed on a FACSCalibur flow cytometer (BD Biosciences, Franklin Lakes, New Jersey). A minimum of 10,000 events were analyzed for each sample, and the dot plots generated after the analysis are presented in Figure S1.

FIGURE 1 Effects of curcumin on HNC cells viability. Kruskal-Wallis test and Dunn's test were applied to the cell viability data, and the IC_{50} values were calculated after a nonlinear regression on the dose-response curves. Graphs (a), (c), and (e) are representations of medians±range. Graphs (b), (d), and (f) are representations of means±SD. Graphs are representations of triplicates. (a, b) Results for the SCC-9 cell line: (a). Curcumin reduced cell viability in a dose-dependent manner, and such reduction was considered significant at (50 μM) (45.4% cell viability, when compared with vehicle-treated cells); (b). Dose-response curve and IC_{50} (40.9 μM). (c, d) Results for the FaDu cell line: (c). Curcumin also reduced cell viability in a dose-dependent manner, with significant difference at (25 μM) and (50 μM) (cell viability values of 48.% and 42.7% respectively, when compared with vehicle-treated cells); (d). Dose-response curve and IC_{50} (24.8 μM). (e, f) Results for the HaCaT cell line: (e). Curcumin resulted in a dose-dependent reduction in cell viability, and the difference to vehicle-treated cells was considered significant at (50 μM) (cell viability of 48.2%); (f). Dose-response curve and IC_{50} (47.3 μM). (g) Tumor Selectivity Indexes (TSIs) were calculated for the tumor cell lines (SCC-9 and FaDu). TSIs higher than 1 indicated that curcumin was selective to the tumor cell lines when compared with the keratinocyte cell line (HaCaT). * = $p < .05$ [Colour figure can be viewed at wileyonlinelibrary.com]

For the cell death assessment, SCC-9 and FaDu cells were seeded into six-well plates at a density of 3.5×10^5 cells/well and incubated overnight. After treatment, cells were collected, washed with PBS, and centrifuged three times to remove the excess of curcumin, and resuspended in culture medium. The CellEvent Caspase-3/7 Green Flow Cytometry Assay Kit (Life Technologies, Carlsbad,

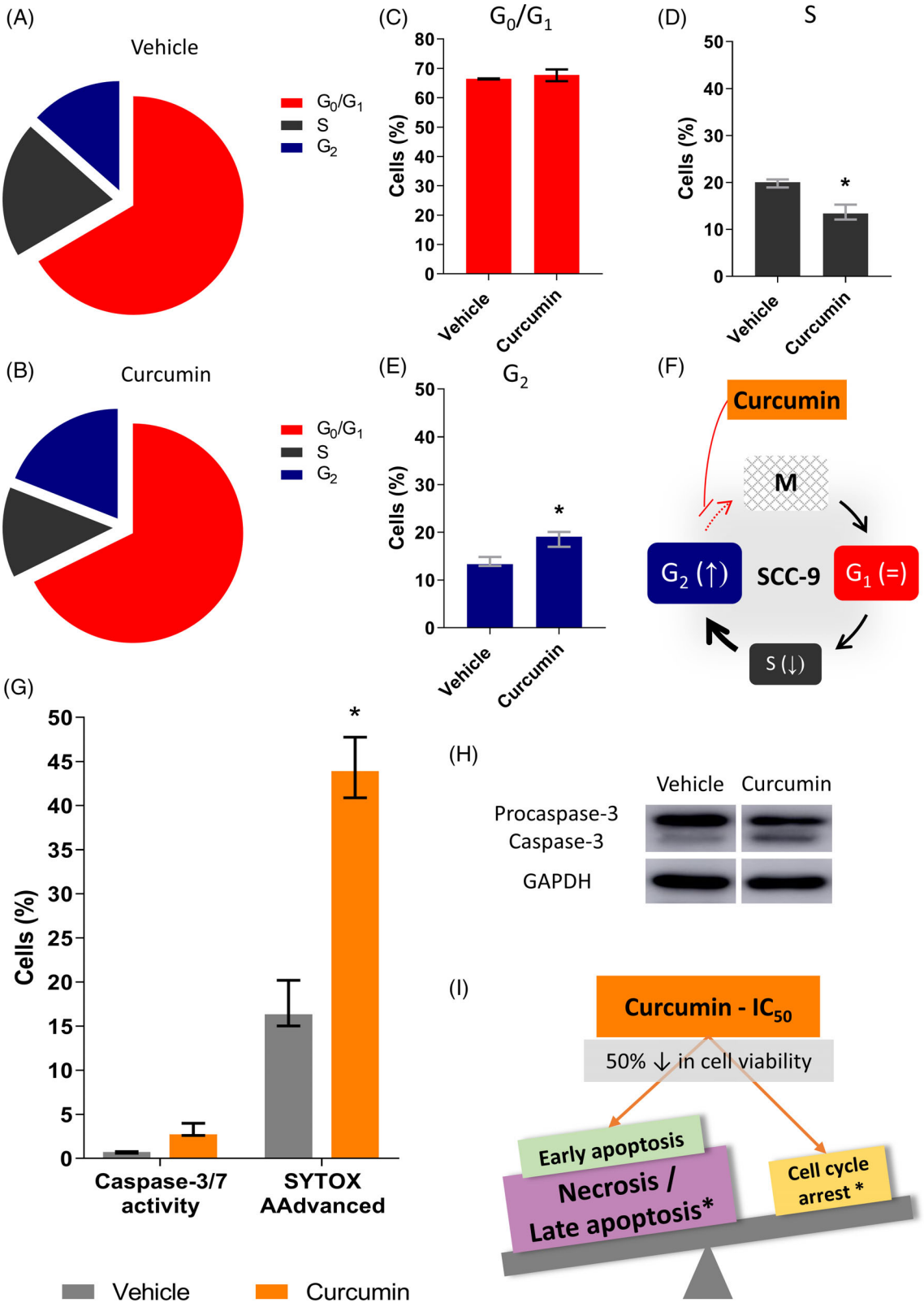

FIGURE 2 Legend on next page.

California—Reference: #C10427) was applied to the cells, according to the manufacturer's instructions. The gate selection was performed with cells that were treated with curcumin but not stained with the CellEvent kit, so that the fluorescence inherent to curcumin would not confound the readings. The samples were assessed on a BD Accuri C6 Plus flow cytometer (BD Biosciences). A minimum of 10,000 events were analyzed for each sample, and the histograms generated after the analysis are presented in Figure S2.

2.5 | Phalloidin assay—Cytoskeleton organization and morphology

SCC-9 and FaDu cells were seeded over glass coverslips placed on the bottom of 12-well plates at a density of 1.6×10^5 cells/well and incubated overnight. After a 24-hr treatment, cells attached to the coverslips were fixated in 4% paraformaldehyde for 10 min and washed with PBS. Cells were permeabilized with 0.5% Triton X-100 for 10 min and washed again. Afterward, cells were incubated with fluorescein phalloidin (1:200) (Invitrogen, Carlsbad, California) for 50 min, protected from light. After washing, the coverslips were mounted with DAPI Fluoromount-G (SouthernBiotech, Birmingham, Alabama). Images were captured with an Axio Imager.M2 microscope (Zeiss, Oberkochen, Germany).

2.6 | qPCR array

SCC-9 and FaDu cells were cultured on $10cm^2$ dishes and incubated overnight. After treatment, cells were washed, and RNA was extracted and purified with TRIzol (Invitrogen) + chloroform (0.2 ml/1 ml TRIzol) and the PureLink RNA Mini Kit (Life Technologies), following the manufacturer's instructions. Samples were treated with the Turbo DNA-free kit (Life Technologies) and stored at −20°C. RNA was quantified and had its quality assessed on a NanoVue Plus spectrophotometer (GE Health Care, Little Chalfont, UK). A total of 2 μg RNA was diluted to the concentration of 0.1 μg/μl, submitted to the reverse transcription reaction using the SuperScript VILO MasterMix (Invitrogen), and stored at −20°C. cDNA samples were diluted to the concentration of 12.5 ng/μl, and 5 μl (12.5 ng cDNA) was mixed to 5 μl TaqMan Fast Advanced Master Mix (Applied Biosystems, Foster City, California) per reaction. This PCR reaction mix was added to each well of custom TaqMan Array 96-well FAST plates (Applied Biosystems) that were designed for this experiment (Table S1). The plates were submitted to the PCR on a StepOnePlus Real-Time PCR System (Applied Biosystems), according to the thermal cycle conditions suggested by the TaqMan MasterMix protocol.

2.7 | Western blot

SCC-9 and FaDu cells were plated and incubated overnight. After treatment, they were washed, lysed, and centrifuged. The protein fraction was collected, quantified, and stored at −80°C. Samples (30 μg-denatured proteins) were loaded in a 10% acrylamide gel and electrophoresed at 100 V. The proteins were then transferred to a PVDF membrane, which was blocked with a 5% blocking solution (milk albumin) for 1 hr and incubated overnight with the primary antibodies (Cell Signaling, Danvers, MA, EUA; Santa Cruz Biotechnology, Dallas, Texas) (Table S2) at 4°C. After incubation, the membrane was washed and incubated with the secondary antibody (Abcam, Cambridge, UK; Santa Cruz Biotechnology) for 1 hr at 4°C. After washing, the membrane was covered with Amersham ECL Prime (GE Healthcare, Little Chalfont, UK) and images were acquired with a chemiluminescence imager (Amersham Imager 600; GE Healthcare). Photos of the full membranes are presented in Figure S3.

2.8 | Statistical analyses

Considering the Gaussian distribution of data, Kruskal-Wallis test and Dunn's test were applied to cell viability results. The IC_{50} values for

FIGURE 2 Effects of curcumin on cell cycle and cell death for the SCC-9 cell line. Mann–Whitney test was applied to all flow cytometry results. Bars are representative of medians±range of triplicates. (a, b) Distribution of vehicle-treated (A) and curcumin-treated (B) cells on the cell cycle: (a). Most of vehicle-treated cells were on phase G_0/G_1 (red—66.5%) and to a lesser extension on phases S (dark grey—20.1%) and G_2 (blue—13.4%); (b). Most curcumin-treated cells remained on phase G_0/G_1 (red—67.7%), and a smaller number of cells were on phases S (dark grey—13.4%) and G_2 (blue—19.1%). (c–e) Comparison between cell populations on phases G_0/G_1, S, and G_2 treated with either vehicle or curcumin: (c). No difference was observed between the populations of vehicle-treated and curcumin-treated cells on phase G_0/G_1; (d). Curcumin significantly reduced the number of cells on phase S; (e). Curcumin significantly increased the number of cells on phase G_2. (f) Summary of the effects of curcumin on the cell cycle of SCC-9 cells: Curcumin reduced the number of cells on phase S and increased the number of cells on phase G_2, which suggests that it induced a cell cycle arrest on the G_2/M transition. (g) Cell death profile after treatment with either vehicle (light grey) or curcumin (orange): Even though curcumin increased the number of cells with active caspase-3/7 in comparison to vehicle (from 0.75 to 2.8%), such difference was not significant. Curcumin significantly increased the number of cells under necrosis/late apoptosis when compared with vehicle (from 16.4 to 44%), considering the nuclear staining with SYTOX AAdvanced. (h) Protein levels of procaspase-3 (upper blots) and its active form, caspase-3 (lower blots): Curcumin reduced the levels of procaspase-3 and increased caspase-3, which suggests that it induced the cleavage of procaspase-3 into caspase-3 in SCC-9 cells. Images of the full membranes are presented in Online Resource 1. (i) Summary of cell cycle and cell death results on the SCC-9 cell line: Curcumin resulted in significant cell cycle arrest and cell death on the SCC-9 cell line. Cell death, especially necrosis/late apoptosis, might be of more relevance than the cell cycle arrest to justify the effects on cell viability (50% reduction, caused by treatment with curcumin at IC_{50} concentration). * = $p < .05$ [Colour figure can be viewed at wileyonlinelibrary.com]

each cell line were estimated through a nonlinear regression on the cell viability dose-response curves. Mann–Whitney test was used on flow cytometry data. Student's *t* test was used to compare the measurements of the nucleus and cytoplasm. Before all assays, the primers and antibodies were validated using positive controls as recommended by the manufacturer. Neither blinding nor randomizing

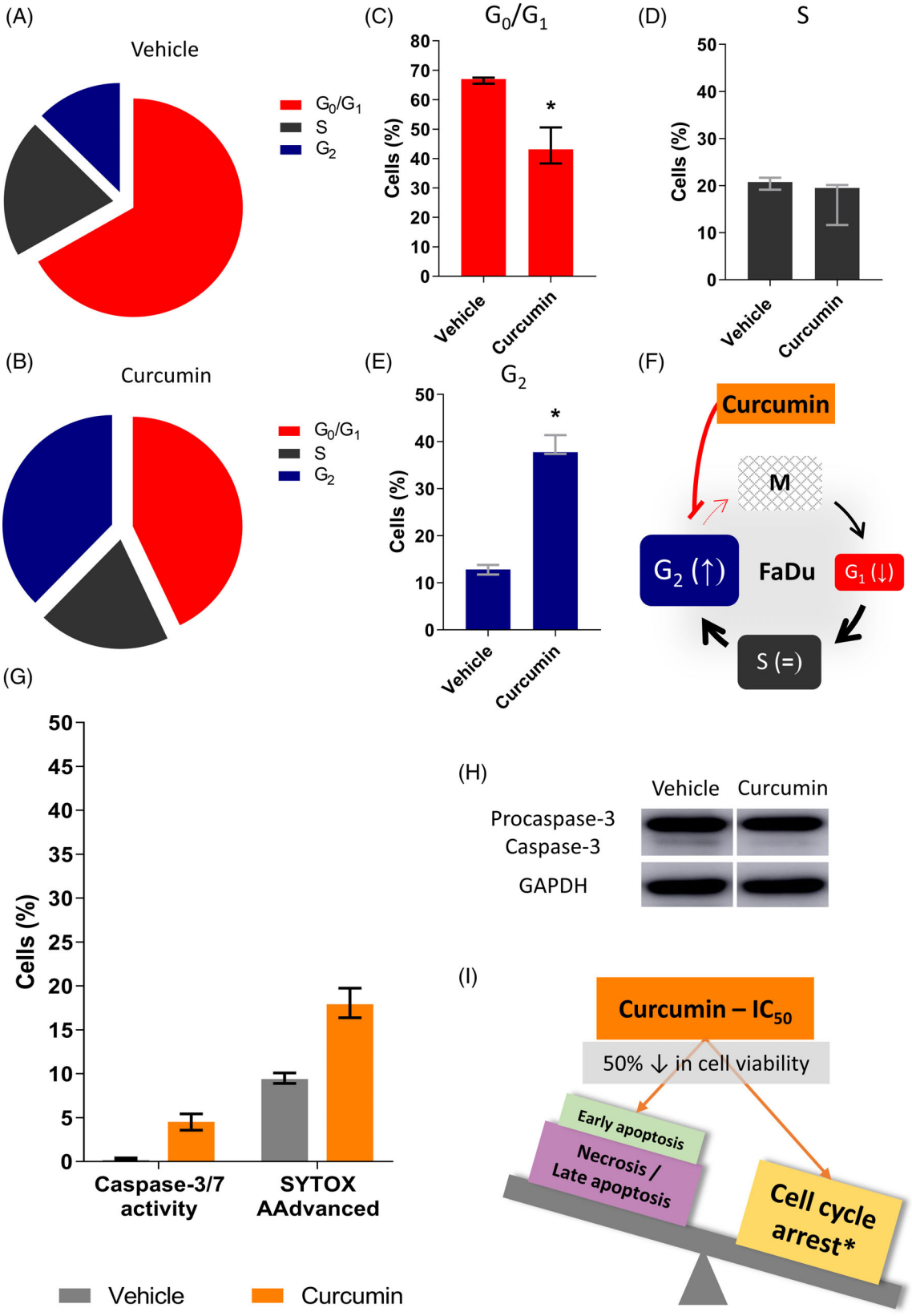

FIGURE 3 Legend on next page.

protocols were applied to the experiments. The software GraphPad Prism 8 (GraphPad Software, Inc., San Diego, California) was used for the analyses and graphs. A p value inferior to .05 was considered significant. Statistical analyses were performed on the results of at least three experiment replicates.

3 | RESULTS

3.1 | Curcumin reduced cell viability in a dose-dependent and selective manner

Aiming to establish IC_{50} values for each cell line, we first conducted an MTT cell viability assay. Cells were treated with curcumin in different concentrations (0.75–50 μM) for 24 and 48 hrs, so that dose-response curves could be defined.

As observed in Figure 1, a reduction in cell viability after 24 hrs of treatment was caused by concentrations higher than 2.5 μM on the tumor cell lines (SCC-9 and FaDu) or 10 μM on the keratinocytes cell line (HaCaT). However, the statistical difference to vehicle-treated cells was only significant with the 50 μM concentration on SCC-9 (median ± range: 45.4 ± 43.7–54.2% vs. vehicle median ± range: 101.3 ± 87.9–110.8%) and HaCaT (median ± range: 48.2 ± 44.9–54.8% vs. vehicle median ± range: 97.6 ± 91.9–110.5%) cells and with the 25 μM and 50 μM concentrations on FaDu cells (median ± range: 48.2 ± 43.7–58.5% and 42.7 ± 37.8–43.9%, respectively, vs. vehicle median ± range: 97.7 ± 89.6–116.8%). Curcumin induced a dose-dependent effect on the three cell lines, although FaDu and SCC-9 cell lines tended to be responsive to lower concentrations of curcumin when compared with HaCaT cells (Figure 1a,c,e).

Based on the 24-hr dose-response curves, IC_{50} values were established for each cell line (Figure 1b,d,f). The FaDu cell line resulted in the lowest IC_{50} (24.8 μM), followed by the SCC-9 cell line (40.9 μM) and the HaCaT cell line with the highest IC_{50} (47.8 μM). TSIs were calculated to define the selectivity of curcumin to the tumor cell lines. A TSI higher than 1 indicates that the treatment is more cytotoxic to the tumor cells than to control cells. Curcumin was selective to SCC-9 (TSI = 1.15) and especially to FaDu (TSI = 1.91) cells, which demonstrates the potential of curcumin as a selectively cytotoxic agent (Figure 1g).

Dose-response curves were defined and IC_{50} values established for cells treated with curcumin for 48 hours. These results did not show any improvement as a consequence of the extended treatment period (Table S3). For this reason, further experiments were conducted only with 24 hrs of treatment.

3.2 | Curcumin induced cell death and cell cycle arrest at the G_2/M phase on SCC-9 and FaDu cells

Considering that a cell cycle arrest is associated with cellular stress and may result in cell death (Diaz-Moralli, Tarrado-Castellarnau, Miranda, & Cascante, 2013), we further investigated the effects of curcumin on the cell cycle distribution of HNC cells. Curcumin significantly reduced the number of SCC-9 cells that were on phase S (1.4-fold decrease; median ± range: 13.4 ± 12.1–15.2% curcumin vs. 20.1 ± 18.9–20.62% vehicle), while increasing the cell population on phase G_2 (1.4-fold increase; median ± range: 19.1 ± 17–20.1% curcumin vs. 13.4 ± 12.9–14.9% vehicle) (Figure 2a–e). Such significant accumulation of cells on phase G_2 indicates that curcumin induced a G_2/M cell cycle arrest, by inhibiting cells to proceed from interphase to mitosis (Figure 2f).

The number of cells undergoing necrosis or late apoptosis (cells with a permeable cell membrane and positive to SYTOX AAdvanced) or early apoptosis (cells with active caspase 3/7) was also investigated. A significant 2.7-fold increase in the number of SCC-9 cells undergoing necrosis/late apoptosis was observed after treatment with curcumin (median ± range: 44 ± 40.9–47.8% curcumin vs. 16.4 ± 15–20.2% vehicle) (Figure 2g). Curcumin also increased the number of early apoptotic SCC-9 cells (3.7-fold increase; median ± range: 2.8 ± 2.6–4% curcumin vs. 0.75 ± 0.6–0.8% vehicle), even though this difference was not

FIGURE 3 Effects of curcumin on cell cycle and cell death for the FaDu cell line. Mann–Whitney test was applied to all flow cytometry results. Bars are representative of medians±range of triplicates. (a, b) Distribution of vehicle-treated (A) and curcumin-treated (B) cells on the cell cycle: (a). Most of vehicle-treated cells were on phase G_0/G_1 (red—67%) and to a lesser extension on phases S (dark grey—20.5%) and G_2 (blue—12.9%). (b). The distribution of curcumin-treated cells in the cell cycle was more homogeneous: most cells remained on G_0/G_1 (red—43.1%), and a smaller number of cells were on phases S (dark grey—19.3%) and G_2 (blue—37.8%). (c–e) Comparison between cell populations on phases G_0/G_1, S, and G_2 treated with either vehicle or curcumin: (c). Curcumin significantly reduced the number of cells on phase G_0/G_1; (d). No difference was observed between the populations of vehicle-treated and curcumin-treated cells on phase S; (e). Curcumin significantly increased the number of cells on phase G_2. (f) Summary of the effects of curcumin on the cell cycle of FaDu cells: Curcumin reduced the number of cells on phase G_0/G_1 and considerably increased the number of cells on phase G_2, which suggests that it induced an important cell cycle arrest on the G_2/M transition. (g) Cell death profile after treatment with either vehicle (light grey) or curcumin (orange): Even though curcumin increased the number of cells under early apoptosis (caspase-3/7 positive) and necrosis/late apoptosis (SYTOX Aadvanced-stained), such differences were not significant. (h) Protein levels of procaspase-3 (upper blots) and its active form, caspase-3 (lower blots): Curcumin did not alter the levels of procaspase-3 and caspase-3 in the FaDu cells. Images of the full membranes are presented in Online Resource 1. (i) Summary of cell cycle and cell death results on the FaDu cell line: Curcumin resulted in significant cell cycle arrest and was not found to induce necrosis nor apoptosis on the FaDu cell line. The cell cycle arrest justifies the effects on cell viability (50% reduction, caused by treatment with curcumin at IC_{50} concentration). * = $p < .05$ [Colour figure can be viewed at wileyonlinelibrary.com]

significant (Figure 2g). Additionally, the western blots presented in Figure 2h indicate that curcumin leads to the cleavage of procaspase-3 into its active form, caspase-3, a protein that works as an apoptosis effector.

In Figure 2i, a schematic representation of these findings is presented. It evidences that the 50% reduction in cell viability that was observed after treating SCC-9 cells with curcumin at IC_{50} concentration is explained by both a cell cycle arrest and the induction of cell

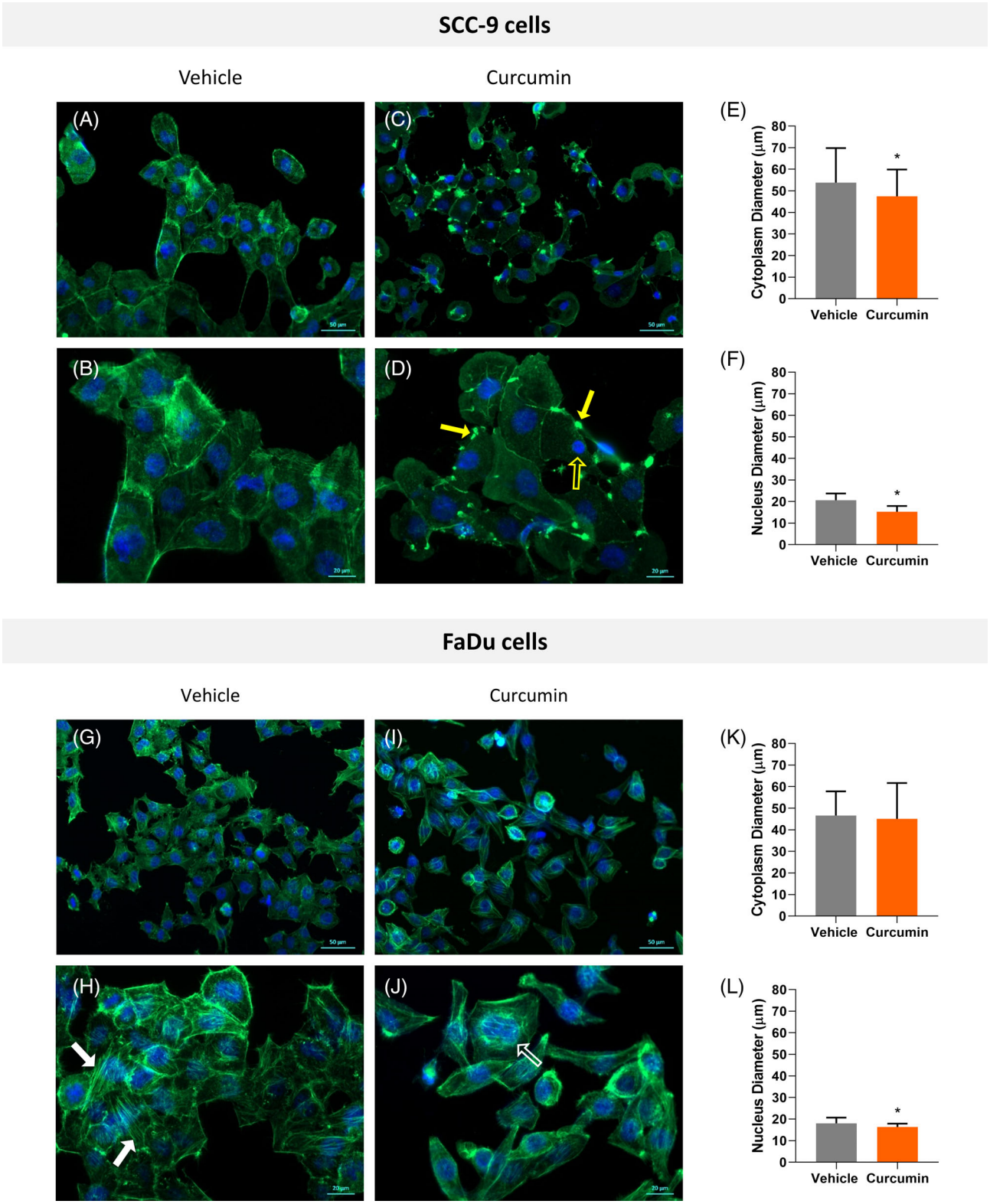

FIGURE 4 Legend on next page.

death. Cell death might be more relevant to justify the effects of curcumin on cell viability, considering that it was more intense than the differences observed in the cell cycle.

Curcumin resulted in a significant threefold increase in the number of FaDu cells on phase G_2 (median ± range: 37.8 ± 37.4–41.4% curcumin vs. 12.9 ± 11.8–13.8% vehicle), while it also caused a 1.6-fold reduction in the cell population on phase G_0/G_1 (median ± range: 43.1 ± 38.4–50.6% curcumin vs. 67 ± 65.5–67.5% vehicle) (Figure 3a–e). Curcumin significantly induced an accumulation of cells on phase G_2, more intensely than on SCC-9 cells, and it indicates a G_2/M cell cycle arrest (Figure 3f). Although curcumin increased considerably the number of FaDu cells undergoing early apoptosis (25-fold increase; median ± range: 4.5 ± 3.6–5.4% curcumin vs. 0.18 ± 0.11–0.42% vehicle) and necrosis/late apoptosis (1.9-fold increase; median ± range: 17.9 ± 16.4–19.8% curcumin vs. 9.4 ± 8.9–10.1% vehicle), this difference was not statistically significant (Figure 3g). No difference in the levels of procaspase-3 or caspase-3 was observed on the western blot assay (Figure 3h).

In Figure 3i, a schematic representation of these results is presented. It suggests that the 50% reduction in cell viability that was observed after treating FaDu cells with curcumin at IC_{50} concentration was mainly explained by a significant cell cycle arrest, even though curcumin tended to induce cell death as well.

3.3 | Curcumin modified the cytoskeleton organization and cell morphology

We also assessed the effects of curcumin on FaDu and SCC-9 cells regarding the actin cytoskeleton organization and cell morphology. It is known that a well-orchestrated remodeling of actin filaments in the cytoskeleton is fundamental to cell motility and migration, differentiation, and proliferation (Fife, McCarroll, & Kavallaris, 2014; Svitkina, 2018). Mutations and aberrant expression of actin and other cytoskeletal proteins are associated with chemotherapy resistance and metastasis in cancer (Fife et al., 2014; Svitkina, 2018). The disruption of the cytoskeleton organization is associated with decreased cell migration and might result in apoptosis (Fife et al., 2014), which are features of interest for a possible cancer therapy agent.

Vehicle-treated cells had their cytoskeleton organized in well-defined f-actin filament networks, consistently distributed across the cytoplasm (Figure 4a,b,g,h). Especially on FaDu cells, the filaments were organized as stress fibers, mostly oriented parallel to the long axis of the cell (Figure 4h). No morphological alteration was observed in vehicle-treated cells.

Curcumin resulted in the disruption of cytoskeleton organization on both cell lines, characterized by the loss of the f-actin networks and a diffuse and granular distribution of actin throughout the cytoplasm (Figure 4c,d,i,j). On SCC-9 cells, it was possible to observe peripherical depositions of actin, with a granular and concentrated aspect (Figure 4d). Morphologically, curcumin induced rounding and flattening of cells, as well as micronucleation and multinucleation in some cells. Curcumin caused a statistically significant reduction in the cytoplasm diameter of SCC-9 cells (mean ± SD: 47.5 ± 12.4 μM curcumin vs. 53.9 ± 16 μM vehicle) and in the nucleus diameter of both SCC-9 (mean ± SD: 15.3 ± 2.6 μM curcumin vs. 20.7 ± 3.1 μM vehicle) and FaDu cells (mean ± SD: 16.3 ± 1.6 μM curcumin vs. 18.1 ± 2.6 μM vehicle) (Figure 4e,f,k,l).

3.4 | Curcumin altered the expression of genes related to the PI3k–AKT–mTOR pathway

The PI3K–AKT–mTOR signaling pathway plays an essential role in keeping the cells growing and proliferating, migrating, and even invading (Murugan, 2019). Knowingly overactivated in the context of oral carcinogenesis, this signaling pathway is associated with increased cell proliferation, evasion of apoptosis, and metastasis, all hallmarks of cancer (Murugan, 2019). A qPCR array was performed to investigate the changes curcumin induces in the expression of genes that are related to the PI3K–AKT–mTOR pathway.

As observed in Figure 5a, a noticeable number of genes had their expression altered by curcumin. A selection of genes whose

FIGURE 4 Effects of curcumin on cytoskeleton organization and cell morphology. Student's *t* test was applied to the morphometric data (e, f, k, and l). Bars are representative of means±SD of 45 measurements of nuclei and cytoplasms of cells in random fields. Green: Phalloidin+FITC; Blue: DAPI. (a, c, g, and i)—20× magnification (scale bars = 50 μm); (b, d, h, and j)—40× magnification (scale bars = 20 μm). (a, b) Vehicle-treated SCC-9 cells: actin filaments are organized in a distinct network, distributed homogeneously throughout the cell cytoplasm. Cytoplasm and nucleus are morphologically normal, as expected. (c, d) Curcumin-treated SCC-9 cells: When compared with vehicle-treated cells, modifications on the cell morphology and the actin filament organization are noticeable. Curcumin induced rounding and flattening of the cells. Actin is distributed in a diffuse and granular pattern in the cytoplasm, and the microfilament organization is lost. Granular depositions of Actin were observed in the periphery of cells (d—solid yellow arrows), as well as micronucleations (d—open yellow arrow). (e, f) Cytoplasm (e) and nucleus (f) diameter measurements: Curcumin induced a significant reduction in the diameter of both cytoplasm (from 53.9 to 47.5 μm) and nucleus (from 20.7 to 15.3 μm) of SCC-9 cells. (g, h) Vehicle-treated FaDu cells: actin filaments are clearly organized into stress fibers (h—solid white arrow), oriented parallel to the long axis of the cells and distributed throughout the cell cytoplasm. Cytoplasm and nucleus are morphologically normal. (i, j) Curcumin-treated FaDu cells: when compared with vehicle-treated cells (g, h), it is possible to observe that the actin filaments organization was kept to a lesser degree, yet in some cells, a complete disorganization of the cytoskeleton is noticed. Curcumin induced rounding and flattening of the cells, which acquire a circular/ovoid appearance. Multinucleation (j—open white arrow) is observed. (k, l) Cytoplasm (k) and nucleus (l) diameter measurements: curcumin induced a significant reduction in the nucleus diameter (from 18.1 to 16.3 μm) of FaDu cells. No difference in the cytoplasm diameter was noticed. * = $p < .05$ [Colour figure can be viewed at wileyonlinelibrary.com]

expression changed the most (fold change >2 or <0.5) is depicted in Figure 5b–c. In SCC-9 cells, the changes in the expression of *PRKCG*, *EGF*, *PLD1*, *RPS6KA1*, *DDIT4*, *RAC1*, *EGFR*, *IRS1*, *STRADB*, *EIF4E*, *ULK1*, *PRKAA1*, *RICTOR*, and *A1BG* were of considerable importance. In FaDu cells, a markedly increased expression of *PRKCG*, *PRKAG2*, *VEGFC*, and *PRKAB1* was noticed.

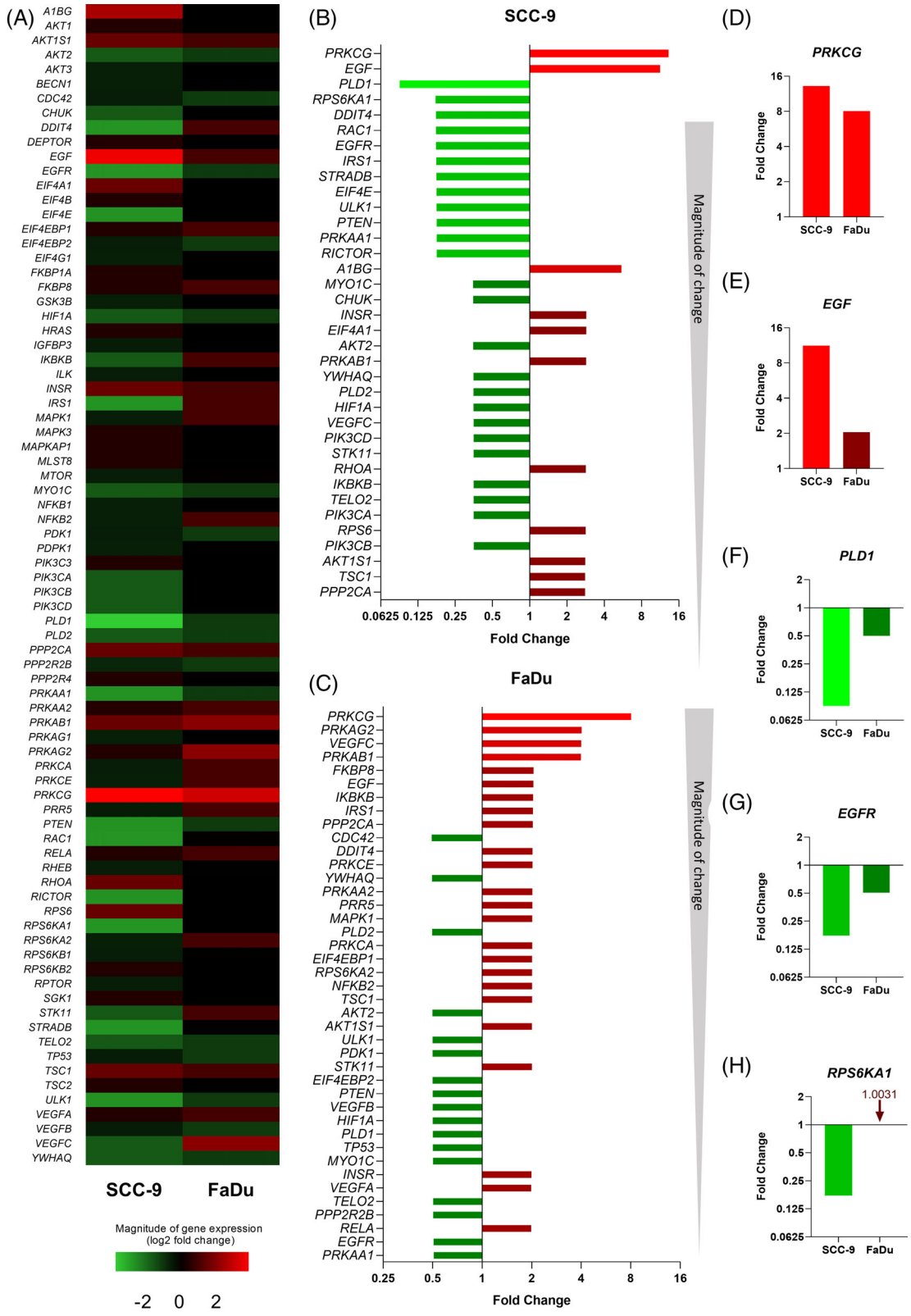

FIGURE 5 Legend on next page.

The gene with the most considerable change in expression on both cell lines was *PRKCG* that had its expression increased 13.2-fold on SCC-9 and eightfold on the FaDu cell line (Figure 5d). An increased expression of *EGF* (11.3-fold change) (Figure 5e) and a decreased expression of *PLD1* (0.089-fold change) (Figure 5f), the second and third most altered genes on SCC-9 cells, were also noteworthy. Other genes that had their expression importantly decreased by curcumin were *EGFR* (Figure 5g), both 0.18-fold and 0.5-fold changes on SCC-9 and FaDu cell lines, respectively), and *RPS6KA1* (Figure 5h) (0.17-fold change on SCC-9).

3.5 | Curcumin downregulated the protein expression of PI3K–AKT–mTOR pathway

The expression of key proteins to the PIK3–AKT–mTOR signaling pathway and their phosphorylation status were assessed through western blot assays, which are presented in Figure 6. The deregulation of the PI3K–AKT–mTOR signaling pathway is pivotal in human oncogenesis, and as a major effector of this signaling pathway, mTOR is widely implicated in cell transformation, proliferation, and survival (Murugan, 2019). On SCC-9 and FaDu cells, curcumin decreased the levels of total and phosphorylated mTOR. PI3K (p110α), AKT, and mTOR were downregulated by curcumin on SCC-9 and FaDu cells, as well as the phosphorylated forms of AKT and mTOR. The downstream effector p70 S6K was not altered by curcumin under the experimental conditions described in this study, but p85 S6K was downregulated on SCC-9 cells.

4 | DISCUSSION

The therapeutic potential of curcumin and other curcuminoids has been thoroughly described, even though concerns regarding their stability, solubility, and bioavailability have been raised, chiefly motivated by the lack of successful results from controlled clinical trials, as reviewed by Nelson et al. (2017). Yet, recent double-blind controlled clinical trials indicate that curcumin improved glycemic factors, hepatic function, and serum cortisol levels in overweight patients (Cicero et al., 2019; Jazayeri-Tehrani et al., 2019), aided lowering cholesterol in hypercholesteremic patients (Ferguson, Stojanovski, MacDonald-Wicks, & Garg, 2018), and decreased triglycerides levels and inflammation in diabetic patients (Adibian et al., 2019). Additionally, there has been an effort to overcome limitations to the clinical use of curcumin, such as its poor bioavailability and solubility. Strategies to improve its delivery (e.g. nanoparticles or liposomes) and to design derivatives and analogs with better therapeutic properties are being developed (Noureddin, El-Shishtawy, & Al-Footy, 2019).

An anticancer drug must act selectively to tumor cells, which is directly linked to the effectiveness of the treatment and to an improved survival and quality of life. Curcumin was selective for FaDu and HaCaT cell lines, when compared with the keratinocytes, which supports its potential as an anticancer agent. Phase I clinical trials with both healthy and cancer patients indicate that treatments with curcumin, even in high daily doses, do not result in severe adverse events (Cheng et al., 2001; Gattoc et al., 2017; Kanai et al., 2013), which suggests that curcumin is safe and does not target uncompromised cells. Additionally, several phase II and III clinical trials are currently under development. A phase III clinical trial (NCT03769766) is being conducted to assess the potential of curcumin in preventing the progression of prostate cancer. Another (NCT02064673) is investigating its effect on recurrence-free survival in prostate cancer patients submitted to radical prostatectomy. Ongoing phase II studies are assessing the association of curcumin with bevacizumab or the FOLFIRI regimen (folinic acid, fluorouracil, and irinotecan) on progression-free survival in colorectal cancer patients with unresectable metastasis (NCT02439385) and the association of curcumin to paclitaxel in advanced breast cancer (NCT03072992).

A significantly increased number of SCC-9 and particularly FaDu cells in the phase G_2 of the cell cycle was observed after treatment with curcumin. The G_2/M cell cycle arrest, caused by curcumin on HNC, is not necessarily a novelty, and was observed on different cell lines in the previous studies (Borges et al., 2017), yet this is the first time it is reported on the SCC-9 and FaDu cell lines.

The increase in the number of SCC-9 and FaDu cells undergoing early apoptosis (active caspase-3/7) was not significant in our study. Even so, the western blot assay indicated that curcumin induced the activation of caspase-3 on the SCC-9 cell line. The integrity of the

FIGURE 5 Effects of curcumin on the expression of genes that are related to the PI3K–AKT–mTOR signaling pathway (qPCR array results). Green indicates that curcumin reduced the gene expression when compared with the vehicle-treated samples. Red indicates that curcumin increased expression. Color values indicate the intensity of the effect curcumin exerted on the gene expression (the lighter the color, the more intense the effect was). Values are expressed as fold changes. No replicate was performed. (a) Heat map depicting the changes curcumin induced in the expression profile of all genes that were assessed on the PCR array. Genes are presented alphabetically. (b, c) Selection of the genes that were altered the most (fold change >2 or <0.5) on SCC-9 (b) and FaDu (c) cells: (b) Curcumin considerably increased the expression of *PRKCG* (13.2-fold change) and *EGF* (11.3-fold change) and decreased the expression of *PLD1* (0.089-fold change) on SCC-9 cells. *RPS6KA1*, *DDIT4*, *RAC1*, *EGFR*, *IRS1*, *STRADB*, *EIF4E*, *ULK1*, *PRKAA1*, and *RICTOR* were also substantially decreased (≈ 0.175-fold change), and *A1BG* increased (5.5-fold change). (c) Curcumin increased *PRKCG* (eightfold change) considerably on FaDu cells, as well as *PRKAG2*, *VEGFC*, and *PRKAB1* (≈fourfold change). (d–f) Comparison of the expression on SCC-9 and FaDu cells of the most altered genes after treatment with curcumin: Curcumin induced a sizeable increased expression of *PRKCG* (d) on both SCC-9 and FaDu cell lines, while such a remarkable change on the expression of *EGF* (e) and *PLD1* (f) was only observed on the SCC-9 cell line. (g, h) Other genes that were importantly altered by curcumin: curcumin reduced the expression of *EGFR* (g) on both cell lines and reduced the expression of *RPS6KA1* (h) on SCC-9 cells [Colour figure can be viewed at wileyonlinelibrary.com]

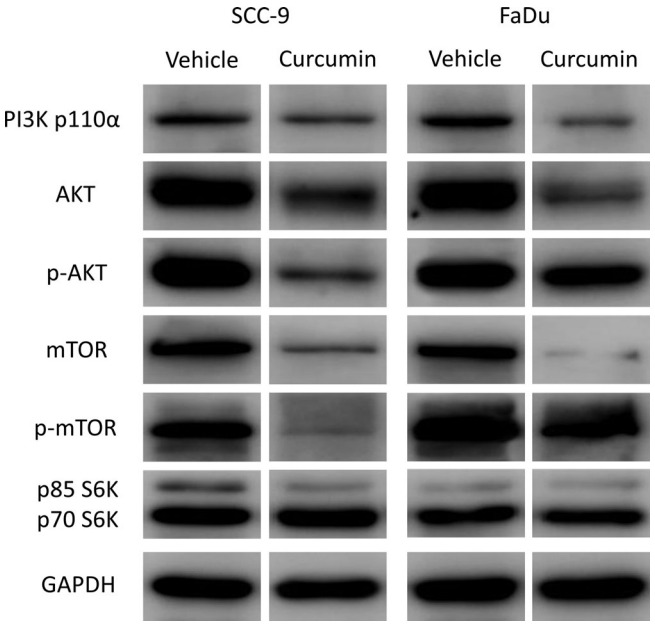

FIGURE 6 Effects of curcumin on the expression of proteins that are related to the PI3K–AKT–mTOR signaling pathway. Curcumin reduced the levels of PI3K, AKT, mTOR, and p85 S6K, all oncogenic proteins, on both SCC-9 and FaDu cell lines. A reduction in the phosphorylated form of AKT (p-AKT) and mTOR (p-mTOR) was also observed, especially on the SCC-9 cell line. Images of the full western blot membranes are presented in Figure S3. The blots here presented are representative of at least three independent replicates for each experimental condition

plasma membrane classically distinguishes necrosis from apoptosis, being the first characterized by a membrane rupture and permeability, and the last by an intact membrane throughout the process (Zhang, Chen, Gueydan, & Han, 2018). However, an insufficient removal of apoptotic cells, which is physiologically promoted by phagocytes, results in a progressive loss of plasma membrane integrity in apoptotic cells, a condition known as late apoptosis or secondary necrosis (Poon, Hulett, & Parish, 2010; Zhang et al., 2018). Considered the absence of mechanisms for dying cells uptake in our experimental set, it is conceivable that, with time, all presumable apoptotic cells would undergo secondary necrosis. In this circumstance, these apoptotic cells would be permeable and susceptible to the SYTOX AAdvanced staining, which might justify the differences between western blot and cell cytometry results regarding cell death.

Remodeling of the cytoskeleton is fundamental for cells to progress through the cell cycle, with specific changes in contractility, protrusion, and adherence being required in each phase (Jones, Zha, & Humphries, 2019). Therefore, a disruption in the cytoskeleton organization, such as observed on the HNC cells, might be related to the cell cycle arrest on phase G_2/M. Even though early apoptosis was not clearly identified in our study, it is associated with cytoskeleton disorganization and cell cycle arrest (Fife et al., 2014). In fact, Chen et al. (2009) reported that curcumin induced on the cytoskeleton of lung adenocarcinoma cells very similar effects to the ones we observed in our study, and the authors linked the cytoskeleton disruption to apoptosis. Nuclear aberrations such as micronucleation and multinucleation are considered signs of genotoxicity, and they are associated with apoptosis (Niero & Machado-Santelli, 2013). Treatment with curcumin resulted in a reduction in the nucleus diameter, observed on both cell lines, as well as micronucleation and multinucleation.

Curcumin induced a noticeable increase in the expression of *EGF* (11.3-fold change), which encodes the epidermal growth factor (EGF), one of the growth factors that trigger the PI3K–AKT–mTOR pathway (Murugan, 2019). Epidermal growth factor receptor (EGFR), on the other hand, was greatly decreased (0.18-fold change). Additionally, curcumin importantly reduced the expression of *RICTOR* (rapamycin-insensitive companion of mTOR—RICTOR), a constituent of mTORC2, on SCC-9 cells. Although curcumin did not alter the expression of the downstream effector p70 S6K nor of its genes (*RPS6KB1* and *RPS6KB2*), it markedly reduced the expression of the p85 S6K protein and its gene *RPS6KA1* (0.17-fold change) on SCC-9 cells. Also noteworthy was the reduced expression of *EIF4E* (0.18-fold change) (eukaryotic translation initiation factor 4E—eIF4E), a transcription factor activated by mTORC1, on SCC-9 cells.

Of all genes that were investigated, *PRKCG* was the one with the most altered expression on both cell lines. The protein kinase C gamma (PKCγ), encoded by *PRKCG*, was believed to be expressed exclusively in neuronal tissues, and its role in oncogenesis is not clear enough (Martiny-Baron & Fabbro, 2007). Even though studies regarding the function of PKCγ in tissues other than neuronal and in the development of cancer are scarce, a few have reported that it is expressed in colon cancer cells (Garczarczyk, Szeker, Galfi, Csordas, & Hofmann, 2010; Parsons & Adams, 2008), prostate cancer cells (Rosenberg & Ravid, 2006), and in the retina (Zhang et al., 2011). Dowling et al. (2017) report that silencing *PRKCG* increased cell proliferation and adhesion in colon cancer cells. In our study, curcumin increased the expression of *PRKCG* 13.2-fold on SCC-9 cells and eightfold on FaDu. Even so, the role of PKCγ on HNC cells still remains elusive.

Although the PKC family has a myriad of functions in different cell types and tissues, it has been traditionally associated with cell transformation and cancer development (Isakov, 2018; Martiny-Baron & Fabbro, 2007). Based on this assumption, many PKC inhibitors underwent clinical trials, even though their success was limited (Isakov, 2018). Recent studies suggest that higher levels of PKCα are positively correlated to improved survival in pancreatic adenocarcinoma patients (Baffi, Van, Zhao, Mills, & Newton, 2019) and that PKCβII is considerably downregulated in colorectal cancer tissues (Dowling et al., 2016). Altogether, these results indicate that PKC isoforms act as tumor suppressors, and that the efforts on cancer therapy should focus on restoring PKC activity, and not on inhibiting it (Isakov, 2018). Even so, it is essential to note that the function of PKC on cancer seems to be tissue- or cell-type specific, and that the expression of PKC isoforms is highly variable (Isakov, 2018).

Our results also indicated that curcumin reduced the expression of *PLD1* and *PLD2* on both cell lines. The reduction of *PLD1* expression was particularly remarkable on SCC-9 cells (0.089-fold change), which suggests that a reduced expression of PLD1 might have aided the reduction in mTOR activity. Phospholipase D (PLD) is an enzyme that is extensively found in a variety of organisms. In humans, the isoforms PLD1 and PLD2

catalyze the production of phosphatidic acid (Brown, Thomas, & Lindsley, 2017). It binds to mTOR and displaces the mTOR-interacting protein (DEPTOR), a mTORC1 endogenous inhibitor, which results in mTORC1 activation and stabilization (Yoon et al., 2015; Laplante & Sabatini, 2012). Increased expression, subcellular mislocalization, and altered catalytic activity of PLD1 and PLD2 have been linked to a variety of cancer types (Laplante & Sabatini, 2012).

As a limitation of this study, we would like to highlight that the qPCR array was planned as an exploratory experiment. An array of genes that had been reported as associated with the PI3K–AKT–mTOR pathway at any degree was considered in the exploratory qPCR array that we performed. As we investigate the changes in a few protein expression, we suggest further studies to demonstrate the function of more proteins related to the PI3K–AKT–mTOR pathway after treatment with curcumin.

In conclusion, this study indicates that curcumin is a promising therapeutic agent because of its potential to inhibit HNC growth and progression. Such effects could be related to the reduced cell viability, cytoskeleton disorganization, cell cycle arrest, and cell death that were observed after treatment with curcumin. Also, we provide some pieces of evidence that curcumin downregulates the PI3K–AKT–mTOR signaling pathway on SCC-9 and FaDu cell lines.

ACKNOWLEDGEMENTS

Dr. Borges was supported by CAPES—Coordination for the Improvement ofHigher Education Personnel, Brazil (88881.187926/2018-01) and CNPq—National Council for Scientific and Technological Development, Brazil (140507/2016-7). Dr. Guerra was also supported by Foundation of the Federal District-FAPDF; (grant 00193.00002099/2018-65) and EDITAL DPI-UnB N04/2019 –(grant 33902001). The authors declare no potential conflicts of interest concerning the authorship and/or publication of this article.

CONFLICT OF INTEREST

The authors declare no conflicts of interest.

ORCID

Gabriel Alvares Borges https://orcid.org/0000-0002-6700-8782
Eliete Neves Silva Guerra https://orcid.org/0000-0002-7622-1550

REFERENCES

Adibian, M., Hodaei, H., Nikpayam, O., Sohrab, G., Hekmatdoost, A., & Hedayati, M. (2019). The effects of curcumin supplementation on high-sensitivity C-reactive protein, serum adiponectin, and lipid profile in patients with type 2 diabetes: A randomized, double-blind, placebo-controlled trial. *Phytotherapy Research*, *33*(5), 1374–1383. https://doi.org/10.1002/ptr.6328

Baffi, T. R., Van, A. N., Zhao, W., Mills, G. B., & Newton, A. C. (2019). Protein kinase C quality control by phosphatase PHLPP1 unveils loss-of-function mechanism in cancer. *Molecular Cell*, *74*(2), 378–392. https://doi.org/10.1016/j.molcel.2019.02.018

Borges, G. A., Rego, D. F., Assad, D. X., Coletta, R. D., De Luca Canto, G., & Guerra, E. N. (2017). In vivo and in vitro effects of curcumin on head and neck carcinoma: A systematic review. *Journal of Oral Pathology and Medicine*, *46*(1), 3–20. https://doi.org/10.1111/jop.12455

Bray, F., Ferlay, J., Soerjomataram, I., Siegel, R. L., Torre, L. A., & Jemal, A. (2018). Global cancer statistics 2018: GLOBOCAN estimates of incidence and mortality worldwide for 36 cancers in 185 countries. *CA: A Cancer Journal for Clinicians*, *68*(6), 394–424. https://doi.org/10.3322/caac.21492

Brown, H. A., Thomas, P. G., & Lindsley, C. W. (2017). Targeting phospholipase D in cancer, infection and neurodegenerative disorders. *Nature Reviews Drug Discovery*, *16*(5), 351–367. https://doi.org/10.1038/nrd.2016.252

Chen, Q., Lu, G., Wang, Y., Xu, Y., Zheng, Y., Yan, L., … Zhou, J. (2009). Cytoskeleton disorganization during apoptosis induced by curcumin in A549 lung adenocarcinoma cells. *Planta Medica*, *75*(8), 808–813. https://doi.org/10.1055/s-0029-1185399

Cheng, A. L., Hsu, C. H., Lin, J. K., Hsu, M. M., Ho, Y. F., Shen, T. S., … Hsieh, C. Y. (2001). Phase I clinical trial of curcumin, a chemopreventive agent, in patients with high-risk or pre-malignant lesions. *Anticancer Research*, *21*(4B), 2895–2900.

Cicero, A. F. G., Sahebkar, A., Fogacci, F., Bove, M., Giovannini, M., & Borghi, C. (2019). Effects of phytosomal curcumin on anthropometric parameters, insulin resistance, cortisolemia and non-alcoholic fatty liver disease indices: A double-blind, placebo-controlled clinical trial. *European Journal of Nutrition*, *59*, 477–483. https://doi.org/10.1007/s00394-019-01916-7

Cramer, J. D., Burtness, B., Le, Q. T., & Ferris, R. L. (2019). The changing therapeutic landscape of head and neck cancer. *Nature Reviews. Clinical Oncology*, *16*(11), 669–683. https://doi.org/10.1038/s41571-019-0227-z

Diaz-Moralli, S., Tarrado-Castellarnau, M., Miranda, A., & Cascante, M. (2013). Targeting cell cycle regulation in cancer therapy. *Pharmacology & Therapeutics*, *138*(2), 255–271. https://doi.org/10.1016/j.pharmthera.2013.01.011

Dowling, C. M., Hayes, S. L., Phelan, J. J., Cathcart, M. C., Finn, S. P., Mehigan, B., … Kiely, P. A. (2017). Expression of protein kinase C gamma promotes cell migration in colon cancer. *Oncotarget*, *8*(42), 72096–72107. https://doi.org/10.18632/oncotarget.18916

Dowling, C. M., Phelan, J., Callender, J. A., Cathcart, M. C., Mehigan, B., McCormick, P., … Kiely, P. A. (2016). Protein kinase C beta II suppresses colorectal cancer by regulating IGF-1 mediated cell survival. *Oncotarget*, *7*(15), 20919–20933. https://doi.org/10.18632/oncotarget.8062

Edwards, R. L., Luis, P. B., Varuzza, P. V., Joseph, A. I., Presley, S. H., Chaturvedi, R., & Schneider, C. (2017). The anti-inflammatory activity of curcumin is mediated by its oxidative metabolites. *The Journal of Biological Chemistry*, *292*(52), 21243–21252. https://doi.org/10.1074/jbc.RA117.000123

Ferguson, J. J. A., Stojanovski, E., MacDonald-Wicks, L., & Garg, M. L. (2018). Curcumin potentiates cholesterol-lowering effects of phytosterols in hypercholesterolaemic individuals. A randomised controlled trial. *Metabolism*, *82*, 22–35. https://doi.org/10.1016/j.metabol.2017.12.009

Fife, C. M., McCarroll, J. A., & Kavallaris, M. (2014). Movers and shakers: Cell cytoskeleton in cancer metastasis. *British Journal of Pharmacology*, *171*(24), 5507–5523. https://doi.org/10.1111/bph.12704

Garczarczyk, D., Szeker, K., Galfi, P., Csordas, A., & Hofmann, J. (2010). Protein kinase Cgamma in colon cancer cells: Expression, Thr514 phosphorylation and sensitivity to butyrate-mediated upregulation as related to the degree of differentiation. *Chemico-Biological Interactions*, *185*(1), 25–32. https://doi.org/10.1016/j.cbi.2010.02.035

Gattoc, L., Frew, P. M., Thomas, S. N., Easley, K. A., Ward, L., Chow, H. S., … Flowers, L. (2017). Phase I dose-escalation trial of intravaginal curcumin in women for cervical dysplasia. *Open Access Journal of Clinical Trials*, *9*, 1–10. https://doi.org/10.2147/OAJCT.S105010

Isakov, N. (2018). Protein kinase C (PKC) isoforms in cancer, tumor promotion and tumor suppression. *Seminars in Cancer Biology*, *48*, 36–52. https://doi.org/10.1016/j.semcancer.2017.04.012

Izzo, A. A. (2020). An updated PTR virtual issue on the pharmacology of the nutraceutical curcumin. *Phytotherapy Research*, *34*(4), 671–673. https://doi.org/10.1002/ptr.6635

Jazayeri-Tehrani, S. A., Rezayat, S. M., Mansouri, S., Qorbani, M., Alavian, S. M., Daneshi-Maskooni, M., & Hosseinzadeh-Attar, M. J. (2019). Nano-curcumin improves glucose indices, lipids, inflammation, and Nesfatin in overweight and obese patients with non-alcoholic fatty liver disease (NAFLD): A double-blind randomized placebo-controlled clinical trial. *Nutrition and Metabolism*, *16*, 8. https://doi.org/10.1186/s12986-019-0331-1

Jones, M. C., Zha, J., & Humphries, M. J. (2019). Connections between the cell cycle, cell adhesion and the cytoskeleton. *Philosophical Transactions of the Royal Society of London. Series B, Biological Sciences*, *374* (1779), 20180227. https://doi.org/10.1098/rstb.2018.0227

Kahkhaie, K. R., Mirhosseini, A., Aliabadi, A., Mohammadi, A., Mousavi, M. J., Haftcheshmeh, S. M., … Sahebkar, A. (2019). Curcumin: A modulator of inflammatory signaling pathways in the immune system. *Inflammopharmacology*, *27*(5), 885–900. https://doi.org/10.1007/s10787-019-00607-3

Kanai, M., Otsuka, Y., Otsuka, K., Sato, M., Nishimura, T., Mori, Y., … Shibata, H. (2013). A phase I study investigating the safety and pharmacokinetics of highly bioavailable curcumin (Theracurmin) in cancer patients. *Cancer Chemotherapy and Pharmacology*, *71*(6), 1521–1530. https://doi.org/10.1007/s00280-013-2151-8

Kotha, R. R., & Luthria, D. L. (2019). Curcumin: Biological, pharmaceutical, nutraceutical, and analytical aspects. *Molecules*, *24*(16), 2930. https://doi.org/10.3390/molecules24162930

Kunnumakkara, A. B., Bordoloi, D., Padmavathi, G., Monisha, J., Roy, N. K., Prasad, S., & Aggarwal, B. B. (2017). Curcumin, the golden nutraceutical: Multitargeting for multiple chronic diseases. *British Journal of Pharmacology*, *174*(11), 1325–1348. https://doi.org/10.1111/bph.13621

Laplante, M., & Sabatini, D. M. (2012). mTOR signaling in growth control and disease. *Cell*, *149*(2), 274–293. https://doi.org/10.1016/j.cell.2012.03.017

Lin, S. R., Chang, C. H., Hsu, C. F., Tsai, M. J., Cheng, H., Leong, M. K., … Weng, C. F. (2020). Natural compounds as potential adjuvants to cancer therapy: Preclinical evidence. *British Journal of Pharmacology*, *177* (6), 1409–1423. https://doi.org/10.1111/bph.14816

Liu, F., Gao, S., Yang, Y., Zhao, X., Fan, Y., Ma, W., … Yu, Y. (2018). Antitumor activity of curcumin by modulation of apoptosis and autophagy in human lung cancer A549 cells through inhibiting PI3K/Akt/mTOR pathway. *Oncology Reports*, *39*(3), 1523–1531. https://doi.org/10.3892/or.2018.6188

Liu, L. D., Pang, Y. X., Zhao, X. R., Li, R., Jin, C. J., Xue, J., … Liu, P. S. (2019). Curcumin induces apoptotic cell death and protective autophagy by inhibiting AKT/mTOR/p70S6K pathway in human ovarian cancer cells. *Archives of Gynecology and Obsterics*, *299*(6), 1627–1639. https://doi.org/10.1007/s00404-019-05058-3

Martiny-Baron, G., & Fabbro, D. (2007). Classical PKC isoforms in cancer. *Pharmacological Research*, *55*(6), 477–486. https://doi.org/10.1016/j.phrs.2007.04.001

Murugan, A. K. (2019). mTOR: Role in cancer, metastasis and drug resistance. *Seminars in Cancer Biology*, *59*, 92–111. https://doi.org/10.1016/j.semcancer.2019.07.003

Nelson, K. M., Dahlin, J. L., Bisson, J., Graham, J., Pauli, G. F., & Walters, M. A. (2017). The essential medicinal chemistry of curcumin. *Journal of Medicinal Chemistry*, *60*(5), 1620–1637. https://doi.org/10.1021/acs.jmedchem.6b00975

Niero, E. L., & Machado-Santelli, G. M. (2013). Cinnamic acid induces apoptotic cell death and cytoskeleton disruption in human melanoma cells. *Journal of Experimental & Clinical Cancer Research*, *32*, 31. https://doi.org/10.1186/1756-9966-32-31

Normando, A. G. C., de Meneses, A. G., de Toledo, I. P., Borges, G. A., de Lima, C. L., Dos Reis, P. E. D., & Guerra, E. N. S. (2019). Effects of turmeric and curcumin on oral mucositis: A systematic review. *Phytotherapy Research*, *33*(5), 1318–1329. https://doi.org/10.1002/ptr.6326

Noureddin, S. A., El-Shishtawy, R. M., & Al-Footy, K. O. (2019). Curcumin analogues and their hybrid molecules as multifunctional drugs. *European Journal of Medicinal Chemistry*, *182*, 111631. https://doi.org/10.1016/j.ejmech.2019.111631

Pagano, E., Romano, B., Izzo, A. A., & Borrelli, F. (2018). The clinical efficacy of curcumin-containing nutraceuticals: An overview of systematic reviews. *Pharmacological Research*, *134*, 79–91. https://doi.org/10.1016/j.phrs.2018.06.007

Parsons, M., & Adams, J. C. (2008). Rac regulates the interaction of fascin with protein kinase C in cell migration. *Journal of Cell Science*, *121*(17), 2805–2813. https://doi.org/10.1242/jcs.022509

Petiti, J., Rosso, V., Lo Iacono, M., Panuzzo, C., Calabrese, C., Signorino, E., … Cilloni, D. (2019). Curcumin induces apoptosis in JAK2-mutated cells by the inhibition of JAK2/STAT and mTORC1 pathways. *Journal of Cellular and Molecular Medicine*, *23*(6), 4349–4357. https://doi.org/10.1111/jcmm.14326

Poon, I. K., Hulett, M. D., & Parish, C. R. (2010). Molecular mechanisms of late apoptotic/necrotic cell clearance. *Cell Death and Differentiation*, *17* (3), 381–397. https://doi.org/10.1038/cdd.2009.195

Rosenberg, M., & Ravid, S. (2006). Protein kinase Cgamma regulates myosin IIB phosphorylation, cellular localization, and filament assembly. *Molecular Biology of the Cell*, *17*(3), 1364–1374. https://doi.org/10.1091/mbc.e05-07-0597

Saadipoor, A., Razzaghdoust, A., Simforoosh, N., Mahdavi, A., Bakhshandeh, M., Moghadam, M., … Mofid, B. (2019). Randomized, double-blind, placebo-controlled phase II trial of nanocurcumin in prostate cancer patients undergoing radiotherapy. *Phytotherapy Research*, *33*(2), 370–378. https://doi.org/10.1002/ptr.6230

Svitkina, T. M. (2018). Ultrastructure of the Actin cytoskeleton. *Current Opinion in Cell Biology*, *54*, 1–8. https://doi.org/10.1016/j.ceb.2018.02.007

Willenbacher, E., Khan, S. Z., Mujica, S. C. A., Trapani, D., Hussain, S., Wolf, D., & Seeber, A. (2019). Curcumin: New insights into an ancient ingredient against cancer. *International Journal of Molecular Sciences*, *20*(8), 1808. https://doi.org/10.3390/ijms20081808

Yoon, M. S., Rosenberger, C. L., Wu, C., Truong, N., Sweedler, J. V., & Chen, J. (2015). Rapid mitogenic regulation of the mTORC1 inhibitor, DEPTOR, by phosphatidic acid. *Molecular Cell*, *58*(3), 549–556. https://doi.org/10.1016/j.molcel.2015.03.028

Zhang, Q., Wang, D., Singh, N. K., Kundumani-Sridharan, V., Gadiparthi, L., Rao, C. M., & Rao, G. N. (2011). Activation of cytosolic phospholipase A2 downstream of the Src-phospholipase D1 (PLD1)-protein kinase C gamma (PKCgamma) signaling axis is required for hypoxia-induced pathological retinal angiogenesis. *The Journal of Biological Chemistry*, *286*(25), 22489–22498. https://doi.org/10.1074/jbc.M110.217786

Zhang, Y., Chen, X., Gueydan, C., & Han, J. (2018). Plasma membrane changes during programmed cell deaths. *Cell Research*, *28*(1), 9–21. https://doi.org/10.1038/cr.2017.133

SUPPORTING INFORMATION

Additional supporting information may be found online in the Supporting Information section at the end of this article.

How to cite this article: GA Borges, ST Elias, B Amorim, et al. Curcumin downregulates the PI3K–AKT–mTOR pathway and inhibits growth and progression in head and neck cancer cells. *Phytotherapy Research*. 2020;34:3311–3324. https://doi.org/10.1002/ptr.6780